

Numerical Simulation of the Spreading Dynamic Responses of the Multibody System with a Floating Base

Zhaobing Jiang^{1*}, Luzhong Shao² and Fei Shao¹

1. College of Field Engineering, PLA University of Science & Technology, Nanjing 210007, China

2. State Key Laboratory of Disaster Prevention & Mitigation of Explosion & Impact, PLA University of Science & Technology, Nanjing 210007, China

Abstract: To simulate the dynamic responses of the multibody system with a floating base when the upper parts spread with a certain sequence and relative speed, the homogeneous matrix method is employed to model and simulate a four-body system with a floating base and the motions are analyzed when the upper parts are spread sequentially or synchronously. The rolling, swaying and heaving temporal variations are obtained when the multibody system is under the conditions of the static water along with the wave loads and the mean wind loads or the single pulse wind loads, respectively. The moment variations of each joint under the single pulse wind load are also gained. The numerical results showed that the swaying of the floating base is almost not influenced by the spreading time or form when the upper parts spread sequentially or synchronously, while the rolling and the heaving mainly depend on the spreading time and forms. The swaying and heaving motions are influenced significantly by the mean wind loads. The single pulse wind load also has influences on the dynamic responses. The torque of joint 3 and joint 4 in the single pulse wind environment may be twice that in the windless environment when the system spreads with 60 s duration.

Keywords: multibody system; Floating base; spreading form; dynamic response; homogeneous matrix method; wave load; wind load

Article ID: 1671-9433(2015)03-0290-12

1 Introduction

Many offshore structures can be modeled as multibody systems. For floating or fully submerged bodies, fluid-structure interactions have to be taken into account. It means that the motion of the system is influenced by the fluid flow, while the flow field is influenced by the motion of the system. Methods to model fluid-structure interactions and applied them to sample problems in the offshore engineering applications have been discussed (Hu and Kashiwagi, 2008; Kim and Kim, 2014; Kral and Kreuzer, 1999; Lee and Choi, 2015; Du *et al.*, 2014; Xia *et al.*, 2008; Zhang *et al.*, 2014).

Some methods are presented to simulate the motion behaviors of the moored floating offshore structures in time domain (Kim *et al.*, 2013; Kreuzer and Wilke, 2002; Li *et al.*, 2013; Wang *et al.*, 2010; Zhang *et al.*, 2012). Some advanced researches about multibody system are done by Kreuzer and his team in recent years (Dostal and Kreuzer, 2013; Kreuzer *et al.*, 2014; Rui *et al.*, 2012). Offloading operations are simulated and analyzed in time domain (de Wilde *et al.*, 2010; Zhao *et al.*, 2014; Woodburn *et al.*, 2003; Zhao *et al.*, 2013) and the systematic evaluations of the hydrodynamics and responses of the multibody system are also performed in FPSO tandem offloading operation (Wang *et al.*, 2010).

Establishing dynamic equations of system, floating crane based on the multibody system dynamics have been studied to simulate the dynamic responses of a suspended heavy cargo and the floating base (Cha *et al.*, 2010; Ellermann and Kreuzer, 2003; Ellermann *et al.*, 2002; Kreuzer *et al.*, 2014). Zhang had made use of the analysis of apparent gravitation and the apparent buoyancy, and the wave rolling moment was derived. The conclusion showed that the motion of the numerous free slipping heavy loads would tend to be synchronous under the restraining of the side-wall bulkhead with time because of the repeating collision (Zhang *et al.*, 2006).

The ro-ro ship is a typical multibody system and the problems of ship safety with regard to the rolling motion of a ro-ro ship in beam waves are studied (Kim and Kim, 2014; Zhang *et al.*, 2006). A parametric investigation was undertaken to identify and quantify the effect of a number of key parameters, such as wave slope and wave frequency, on the capsizing conditions of a ship. And nonlinear response of ship was determined in the frequency domain (Surendran *et al.*, 2005). Jang had derived the nonlinear dynamics of ship-mounted crane in order to reduce payload pendulation of the ship-mounted crane and a control method using T-S fuzzy model was proposed (Jang *et al.*, 2012).

Legnani *et al.* (1996a; 1996b) have presented a new approach to the kinematic and dynamic analysis of rigid body systems in the form of a consistent method employing 4×4 matrices (Legnani *et al.*, 1996a; 1996b). It could be considered a powerful extension of the well-known method

Received date: 2014-07-29.

Accepted date: 2014-11-19.

Foundation item: Supported by the National Natural Science Foundation of China (Grant No. 51009147) and Major State Basic Research Development Program of China (973 Program) (Grant Nos. 2014CB046801 and 2014CB046804).

*Corresponding author Email: owen9020@126.com

of homogeneous transformations proposed by Denavit and Hartenberg (1955). New matrices were introduced to describe the velocity and the acceleration, the momentum, the inertia of bodies and the actions (forces and torques) applied to them. Each matrix contains both the angular and the linear terms. Thus the “usual” kinematic and dynamic relations could be rewritten, halving the number of equations. The resulting notation and expressions are simple, and are very suitable for computer applications. Based on this method, Jiang *et al.* (2010) have studied the dynamic responses of the floating bridge subjected to fast and heavy loads and of the floating multibody spreading in waves.

In this paper, the homogeneous matrix is introduced and developed to derive the kinematic and dynamic equations of the multibody system with a floating base. The dynamic responses of this multibody system are numerically simulated when the multibody system spreads in the environment of the static water surface, the waves and the winds, respectively. Finally, the results of the simulations are concluded and some suggestions are given for the spreading of the multibody system with a floating base in various environments listed in this paper.

2 Homogenous matrix method

Referring to the homogenous matrix method, the kinematics of a multibody system could be described by three 4×4 matrices. The matrices are the position matrix M , the velocity matrix W and the acceleration matrix H . The pose of a rigid body with respect to the absolute reference frame could be represented by the position matrix:

$$M_{0,1} = \begin{bmatrix} R_{0,1} & t_{0,1} \\ 0 & 0 & 0 & 1 \end{bmatrix} = \begin{bmatrix} x_x & y_x & z_x & t_x \\ x_y & y_y & z_y & t_y \\ x_z & y_z & z_z & t_z \\ 0 & 0 & 0 & 1 \end{bmatrix} \quad (1)$$

where the 3×1 vector $t_{0,1}$ is the position of the origin of the frame (1) in the absolute reference frame (0), while the 3×3 submatrix $R_{0,1}$ is the orthogonal rotation matrix describing the orientation of frame (1) with respect to frame (0). As to the three frames (i), (j) and (k), the position matrix satisfies the relation

$$M_{i,k} = M_{ij} M_{j,k} \quad (2)$$

Apparently, the above formula is the relative transform relation of the position matrix.

The angular and linear velocity of a rigid body with respect to a reference frame could be represented by the velocity matrix:

$$W = \begin{bmatrix} 0 & -\omega_z & \omega_y & v_x \\ \omega_z & 0 & -\omega_x & v_y \\ -\omega_y & \omega_x & 0 & v_z \\ 0 & 0 & 0 & 0 \end{bmatrix} = \begin{bmatrix} \underline{\omega} & v_0 \\ 0 & 0 & 0 & 0 \end{bmatrix} \quad (3)$$

where $\underline{\omega}$ is the angular velocity of a rigid body and v_0 is the velocity of the point. Due to the velocity of a rigid body

is combined by the linear velocity $v_0 = [v_x, v_y, v_z]$ and angular velocity $\underline{\Omega} = [\omega_x \ \omega_y \ \omega_z]^T$, the velocity of a point at the rigid body could be obtained as

$$\dot{P} = WP = \begin{bmatrix} \dot{x}_p \\ \dot{y}_p \\ \dot{z}_p \\ 0 \end{bmatrix} = \begin{bmatrix} \underline{\omega} & v_0 \\ 0 & 0 & 0 & 0 \end{bmatrix} \begin{bmatrix} x_p \\ y_p \\ z_p \\ 1 \end{bmatrix} \quad (4)$$

It is easy to verify that the above equation is a matrix formulation of the usual vector formula $v_p = v_0 + \omega \times (P - O)$. Similarly, the relative acceleration of a rigid body with respect to a reference frame can be combined by the linear acceleration a_0 and angular acceleration $\underline{\dot{\Omega}}$. Therefore, the relative acceleration of a rigid body with respect to a reference frame can be indicated by the acceleration matrix H , as

$$H = \dot{W} + W^2 = \begin{bmatrix} G & a_0 \\ 0 & 0 & 0 & 0 \end{bmatrix} \quad (5)$$

where the 3×3 submatrix $G = \underline{\dot{\omega}} + \underline{\omega}^2$, a_0 is the acceleration of the pole with respect to the reference frame. It obviously yields that $\underline{\dot{\omega}} = (G - G^T)/2$ and $\underline{\omega}^2 = (G + G^T)/2$. The acceleration \ddot{P} of a point P at the rigid body is

$$\ddot{P} = HP = \begin{bmatrix} \ddot{x}_p \\ \ddot{y}_p \\ \ddot{z}_p \\ 0 \end{bmatrix} = \begin{bmatrix} G & a_0 \\ 0 & 0 & 0 & 0 \end{bmatrix} \begin{bmatrix} x_p \\ y_p \\ z_p \\ 1 \end{bmatrix} \quad (6)$$

Similarly, the above equation can be obtained by the dynamic vector formulation:

$$a_p = a_0 + \underline{\dot{\omega}} \times (P - O) + \underline{\omega} \times (\underline{\omega} \times (P - O))$$

Obviously, the values of the matrices including velocity matrix and acceleration matrix are strictly dependent on the reference frame. As to two different reference frames (r) and (s), the same rigid body’s velocity and acceleration at the absolute reference frame must be identical. Therefore, some close relations are existed between them. The formulations of velocity and acceleration matrix at different reference frames could be written as

$$W_{(r)} = M_{r,s} W_{(s)} M_{r,s}^{-1} \quad (7)$$

$$H_{(r)} = M_{r,s} H_{(s)} M_{r,s}^{-1} \quad (8)$$

where $M_{r,s}$ is the position matrix of the reference frame (s) with respect to frame (r). The above equations are the transformation formulas of the velocity and acceleration matrix at different reference frames.

Furthermore, three new matrices are introduced to develop the dynamic analysis of a rigid body system, and they are the action matrix Φ , the momentum matrix Γ and the inertial matrix J .

The forces and torques applied to rigid body k are

represented by the skew-symmetric action matrix Φ_k , as

$$\Phi_k = \begin{bmatrix} \underline{c} & \underline{f} \\ -\underline{f}^T & 0 \end{bmatrix} = \begin{bmatrix} 0 & -c_z & c_y & f_x \\ c_z & 0 & -c_x & f_y \\ -c_y & c_x & 0 & f_z \\ -f_x & -f_y & -f_z & 0 \end{bmatrix} \quad (9)$$

where \underline{f} is the resultant of forces, while \underline{c} is the torques with respect to the origin of the reference frame.

Similarly, the angular and linear momentum of k rigid body with respect to a reference frame may be described by the skew-symmetric momentum matrix Γ_k , as

$$\Gamma_k = \begin{bmatrix} \underline{\gamma} & \underline{\rho} \\ -\underline{\rho}^T & 0 \end{bmatrix} = \begin{bmatrix} 0 & -\gamma_z & \gamma_y & \rho_x \\ \gamma_z & 0 & -\gamma_x & \rho_y \\ -\gamma_y & \gamma_x & 0 & \rho_z \\ -\rho_x & -\rho_y & -\rho_z & 0 \end{bmatrix} \quad (10)$$

where $\underline{\gamma}$ is the angular momentum of rigid body k with respect to the origin of a reference frame and $\underline{\rho} = m[v_{x_g} \ v_{y_g} \ v_{z_g}]^T$ is the linear momentum of the body, while $[v_{x_g} \ v_{y_g} \ v_{z_g}]^T$ is the linear velocity of the centroid of the body and m is the mass of the body.

The mass distribution of rigid body k can be represented by a symmetry inertial matrix J_k , as

$$J_k = \begin{bmatrix} \underline{J} & \underline{q} \\ \underline{q}^T & m \end{bmatrix} = \begin{bmatrix} I_{xx} & I_{xy} & I_{xz} & q_x \\ I_{xy} & I_{yy} & I_{yz} & q_y \\ I_{xz} & I_{yz} & I_{zz} & q_z \\ q_x & q_y & q_z & m \end{bmatrix} \quad (11)$$

where $\underline{q} = m[x_{x_g} \ x_{y_g} \ x_{z_g}]^T$ is the product of the mass by the center of the position of the rigid body. The inertial matrix \underline{J} is different from the usual inertial matrix, so this inertial matrix is also called pseudo inertial matrix.

The elements of the submatrix \underline{J} are defined as:

$$I_{xx} = \int x^2 dm \quad I_{yy} = \int y^2 dm \quad I_{zz} = \int z^2 dm \\ I_{xy} = \int xy dm \quad I_{xz} = \int xz dm \quad I_{yz} = \int yz dm$$

The transformation relations of matrix Φ_k , Γ_k and J_k with respect to given two reference frames are listed below:

$$\Phi_{k(r)} = \underline{M}_{r,s} \Phi_{k(s)} \underline{M}_{r,s}^T \quad (12)$$

$$\Gamma_{k(r)} = \underline{M}_{r,s} \Gamma_{k(s)} \underline{M}_{r,s}^T \quad (13)$$

$$J_{k(r)} = \underline{M}_{r,s} J_{k(s)} \underline{M}_{r,s}^T \quad (14)$$

Based on the kinematic and dynamic matrices of homogenous matrix method, it is easily verified that the Newton Law at an inertial reference frame (0) can be represented by

$$\Phi_{k(0)} = H_{0,k} J_{k(0)} - J_{k(0)} H_{0,k}^T \quad (15)$$

The operator skew is defined for any square matrix X or tensor X to simplify the deduction of some formulas. The Eqn.(15) can be written as

$$\Phi_{k(0)} = \text{skew}[H_{0,k} J_{k(0)}] \quad (16)$$

Similarly, the momentum equation can be written as

$$\Gamma_{k(0)} = \text{skew}[W_{0,k} J_{k(0)}]. \quad (17)$$

For the multibody system, the kinematic equation may be compactly written as follows:

$$\sum_k [-\text{skew}[H_{0,k} J_{k(0)}] + \Phi_{k(0)}] = [\mathbf{0}] \quad (18)$$

and the detailed theory about homogenous method of the multibody system can refer to the papers written by Legnani et al. (1996a).

3 Governing dynamic equations and calculation parameters

The multibody system with a floating base investigated in this paper is shown in Fig. 1. When the upper parts, as the rigid bodies 2–4 in Fig. 1(a), spread on the water surface, their motions may excite the kinematic and dynamic responses of the floating base. Fig. 1(a) and Fig. 1(b) are the no spreading and the complete spreading states, respectively. Rigid body 1 is the floating base, and rigid bodies 2 and 4 are the upper parts whose mass could not be ignored, while the upper part rigid body 3 is the joint part whose mass could be ignored. The relative speeds of the upper parts can be given in advance and are provided by the joint actuators. The forces of the actuators of all joints are internal and they do not appear in the dynamical equations explicitly. The homogeneous matrix method is feasible for six degrees of freedom, but only the planar simulations are given in this paper and the responses of the multibody system may be simplified to 2D space. If the motions of upper parts are given and all of the external forces are known, the dynamic response of this system on the 2D space will be solved by employing the homogenous matrix method and Eq. (18).

When the multibody system with a floating base spreads on the water surface, two spreading orders are employed: sequential or synchronous. The order of sequential spreading is that the joint part 3 and rigid body 4 are regarded as a whole part and turning 90° with respect to rigid body 1. Then the joint part 3 has no motion with respect to rigid body 1 and rigid body 4 turns 90° with respect to rigid body 3. Finally rigid body 2 turns 180° with respect to rigid body 1. The order of synchronous spreading is that the joint part 3 and rigid body 4 are regarded as a whole part and turning 90° with respect to rigid body 1, then the joint part 3 has no motion with respect to rigid body 1 and rigid body 4 with respect to joint part 3 and rigid body 2 with respect to rigid body 1 turn 90° synchronously.

Based on the 2D space diagram of the multibody system with a floating base, four local coordinates are defined as Fig. 2.

When the upper parts of the multibody system spread in the 2D space, the responses of this system include three degrees: swaying, heaving and rolling. The dynamic responses of this multibody system and then the forces and

torques applied on the joints could be numerically simulated by employing the homogenous method.

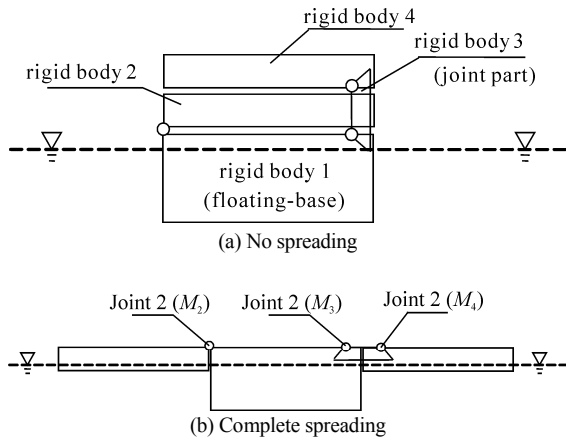


Fig. 1 The multibody system with a floating base

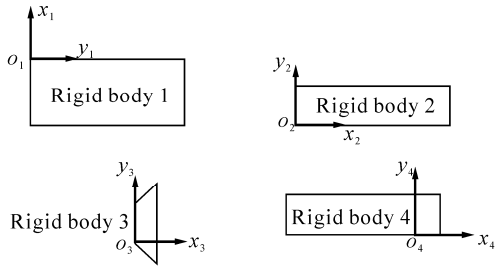


Fig. 2 The local coordinates for all parts of the multibody system

Besides the internal driven torques and pulling forces, which are not included in the Eq. (18) explicitly, the forces acted on the multibody system include the gravity and fluid reactions due to the motions of the multibody system. The fluid forces include the hydrostatic restoring force, the buoyancy, the fluid dynamic force, the wave load and the wind load, etc. As shown in Fig. 1, the fluid forces acted on the rigid bodies 1–4 include static water restoring forces Φ_{FS_i} ($i=1,2,3,4$), static buoyancies Φ_{FB_i} ($i=1,2,3,4$), dynamic fluid forces Φ_{FD_i} ($i=1,2,3,4$) (Shen *et al.*, 2003) and the gravity Φ_{gi} ($i=1,2,3,4$). If the wave loads Φ_{FWA_i} ($i=1,2,3,4$) or wind loads Φ_{FWL_i} ($i=1,2,3,4$) are considered, the corresponding forces may be included at the dynamic equations, see sections 5 and 6. Based on the Eq. (10), the dynamic equation of this multibody system with a floating base can be presented as follows:

$$\sum_{i=1}^4 [\Phi_{FS_i} + \Phi_{FB_i} + \Phi_{FD_i} + \Phi_{gi} - \text{skew}(\mathbf{H}_{0,i} \cdot \mathbf{J}_{i(0)})] = [\mathbf{0}] \quad (19)$$

From the above equation the follow can be obtain:

$$\sum_{i=1}^4 [\Phi_{FS_i} + \Phi_{FB_i} + \Phi_{FD_i} + \Phi_{gi}] = \sum_{i=1}^4 \text{skew}(\mathbf{H}_{0,i} \cdot \mathbf{J}_{i(0)}) \quad (20)$$

By deploying the right side of the above equation the following is obtained:

$$\begin{aligned} & \sum_{i=1}^4 \text{skew}(\mathbf{H}_{0,i} \cdot \mathbf{J}_{i(0)}) = \\ & \text{skew}(\mathbf{H}_{0,1} \cdot \mathbf{J}_{1(0)} + \mathbf{H}_{0,2} \cdot \mathbf{J}_{2(0)} + \mathbf{H}_{0,3} \cdot \mathbf{J}_{3(0)} + \mathbf{H}_{0,4} \cdot \mathbf{J}_{4(0)}) = \\ & \text{skew} \left\{ (\mathbf{W}_{0,1}^2 + \dot{\mathbf{W}}_{0,1}) \cdot \mathbf{J}_{1(0)} + \right. \\ & \left. [(\mathbf{W}_{0,1}^2 + \dot{\mathbf{W}}_{0,1}) + \mathbf{H}_{1,2(0)} + 2 \cdot \mathbf{W}_{0,1} \cdot \mathbf{W}_{1,2(0)}] \cdot \mathbf{J}_{2(0)} + \right. \\ & \left. [(\mathbf{W}_{0,1}^2 + \dot{\mathbf{W}}_{0,1}) + \mathbf{H}_{1,3(0)} + 2 \cdot \mathbf{W}_{0,1} \cdot \mathbf{W}_{1,3(0)}] \cdot \mathbf{J}_{3(0)} + \right. \\ & \left. [(\mathbf{W}_{0,1}^2 + \dot{\mathbf{W}}_{0,1}) + \mathbf{H}_{1,3(0)} + 2 \cdot \mathbf{W}_{0,1} \cdot \mathbf{W}_{1,3(0)} + \right. \\ & \left. \mathbf{H}_{3,4(0)} + 2 \cdot \mathbf{W}_{0,3} \cdot \mathbf{W}_{3,4(0)}] \cdot \mathbf{J}_{4(0)} \right\} \end{aligned} \quad (21)$$

Placing the terms including $\dot{\mathbf{W}}_{0,1}$ on the right side of the equation and the others on the left side the following can be obtained:

$$\begin{aligned} & \text{skew} \left\{ \mathbf{W}_{0,1}^2 \cdot \mathbf{J}_{1(0)} + (\mathbf{W}_{0,1}^2 + \mathbf{H}_{1,2(0)} + 2 \cdot \mathbf{W}_{0,1} \cdot \mathbf{W}_{1,2(0)}) \cdot \mathbf{J}_{2(0)} + \right. \\ & (\mathbf{W}_{0,1}^2 + \mathbf{H}_{1,3(0)} + 2 \cdot \mathbf{W}_{0,1} \cdot \mathbf{W}_{1,3(0)}) \cdot \mathbf{J}_{3(0)} + \\ & (\mathbf{W}_{0,1}^2 + \mathbf{H}_{1,3(0)} + 2 \cdot \mathbf{W}_{0,1} \cdot \mathbf{W}_{1,3(0)} + \mathbf{H}_{3,4(0)} + \\ & \left. 2 \cdot \mathbf{W}_{0,3} \cdot \mathbf{W}_{3,4(0)}) \cdot \mathbf{J}_{4(0)} \right\} - \sum_{i=1}^4 (\Phi_{FS_i} + \Phi_{FB_i} + \Phi_{FD_i} + \Phi_{gi}) = \end{aligned} \quad (22)$$

$$\begin{aligned} & \text{skew}(-\dot{\mathbf{W}}_{0,1} \cdot \mathbf{J}_{1(0)} - \dot{\mathbf{W}}_{0,1} \cdot \mathbf{J}_{2(0)} - \dot{\mathbf{W}}_{0,1} \cdot \mathbf{J}_{3(0)} - \dot{\mathbf{W}}_{0,1} \cdot \mathbf{J}_{4(0)}) = \\ & \text{skew}(-\dot{\mathbf{W}}_{0,1} \cdot \mathbf{J}_{tot}) \end{aligned}$$

where $\mathbf{J}_{tot} = \mathbf{J}_{1(0)} + \mathbf{J}_{2(0)} + \mathbf{J}_{3(0)} + \mathbf{J}_{4(0)}$.

Let:

$$\begin{aligned} \mathbf{H}_{0,1}^* &= \mathbf{W}_{0,1}^2 \\ \mathbf{H}_{0,2}^* &= \mathbf{H}_{0,1}^* + \mathbf{H}_{1,2(0)} + 2 \cdot \mathbf{W}_{0,1} \cdot \mathbf{W}_{1,2(0)} \\ \mathbf{H}_{0,3}^* &= \mathbf{H}_{0,1}^* + \mathbf{H}_{1,3(0)} + 2 \cdot \mathbf{W}_{0,1} \cdot \mathbf{W}_{1,3(0)} \\ \mathbf{H}_{0,4}^* &= \mathbf{H}_{0,3}^* + \mathbf{H}_{3,4(0)} + 2 \cdot \mathbf{W}_{0,3} \cdot \mathbf{W}_{3,4(0)} \end{aligned}$$

and the following can be obtained:

$$\begin{aligned} & \text{skew}(\mathbf{H}_{0,1}^* \cdot \mathbf{J}_{1(0)} + \mathbf{H}_{0,2}^* \cdot \mathbf{J}_{2(0)} + \mathbf{H}_{0,3}^* \cdot \mathbf{J}_{3(0)} + \mathbf{H}_{0,4}^* \cdot \mathbf{J}_{4(0)}) - \\ & \sum_{i=1}^4 (\Phi_{FS_i} + \Phi_{FB_i} + \Phi_{FD_i} + \Phi_{gi}) = \text{skew}(-\dot{\mathbf{W}}_{0,1} \cdot \mathbf{J}_{tot}) \end{aligned} \quad (23)$$

where $\mathbf{H}_{0,1}^*$, $\mathbf{H}_{0,2}^*$, $\mathbf{H}_{0,3}^*$ and $\mathbf{H}_{0,4}^*$ are the “local” acceleration matrices of rigid bodies 1–4, respectively.

After solving Eq. (23), $\dot{\mathbf{W}}_{0,1}$ is obtained. Therefore the absolute acceleration matrices of all rigid bodies can be obtained as follows:

$$\begin{aligned} \mathbf{H}_{0,1} &= \mathbf{H}_{0,1}^* + \dot{\mathbf{W}}_{0,1} \\ \mathbf{H}_{0,2} &= \mathbf{H}_{0,2}^* + \dot{\mathbf{W}}_{0,1} \\ \mathbf{H}_{0,3} &= \mathbf{H}_{0,3}^* + \dot{\mathbf{W}}_{0,1} \\ \mathbf{H}_{0,4} &= \mathbf{H}_{0,4}^* + \dot{\mathbf{W}}_{0,1} \end{aligned}$$

Thus the acceleration matrices of rigid body 1 and other bodies can be obtained. By means of the time integral, the whole spreading dynamic responses of the multibody system with a floating base could be simulated in time domain.

The mass of rigid body 3 or joint part 3 is infinitesimal

with respect to other rigid bodies and it can be ignored. The parameters of the sizes and the centers of gravity of the rigid bodies are listed in Table 1. B , H , L and h are the width, height, length and the height of center of gravity, respectively, in the local coordination defined in Fig. 2.

Supposing the mass distribution of all parts is uniform in the 2D space, the mass and moment of inertia may be calculated as shown in Table 2.

Table 1 The sizes and the heights of centroid of each part in local coordination

Rigid body	B/m	H/m	L/m	h/m
1	3.3	1.64	13	0.491
2 & 4	3.3	0.88	13	0.350

Table 2 The mass and moment of inertia of the floating base multibody

Rigid body	M/kg	$I_{xx}/(kg \cdot m^{-1})$	$I_{yy}/(kg \cdot m^{-1})$	$I_{zz}/(kg \cdot m^{-1})$
1	2.7×10^4	1.85×10^4	7.71×10^3	3.96×10^5
2 & 4	6.5×10^3	7.61×10^3	1.57×10^3	9.83×10^4

4 Numerical results of the spreading on the static water surface

The dynamic responses of the multibody system with a floating base spreading on the static water surface can be solved using Eq. (23). The temporal swaying variation of the floating base is shown in Fig. 3(a) when the upper parts spread sequentially. The total time for the multibody system to completely spread is 15, 30, 60 and 90 s, respectively. The maximum swaying displacement of the floating base is about 0.54 m for all cases and the spreading time has no influence on it. The maximum value is presented near the location when the rigid body 4 spreads entirely. Note that the x coordination is normalized as T for the convenience of comparison among various cases with different spreading time.

The temporal heaving variation of the floating base is shown in Fig. 3(b). It shows the maximum heaving value with sequential spreading has close relation to the spreading time. The positive maximum heaving displacements are 0.228 m and 0.164 m and the negative ones are -0.085 m and -0.022 m when the upper parts spread in 15 s and 90 s, respectively. It indicates that the longer the spreading time is, the less the impacts of the inertial force is on the spreading process and the dynamic responses.

The temporal rolling variation of the floating base is shown in Fig. 3(c). It demonstrates the maximum rolling angle is presented when the rigid body 4 and joint part 3 are spreading on the half time point with respect to rigid 1. The longer the upper parts spread sequentially, the smoother the rolling responses are. However, the maximum value of the rolling angles does not decrease when the spreading time is longer.

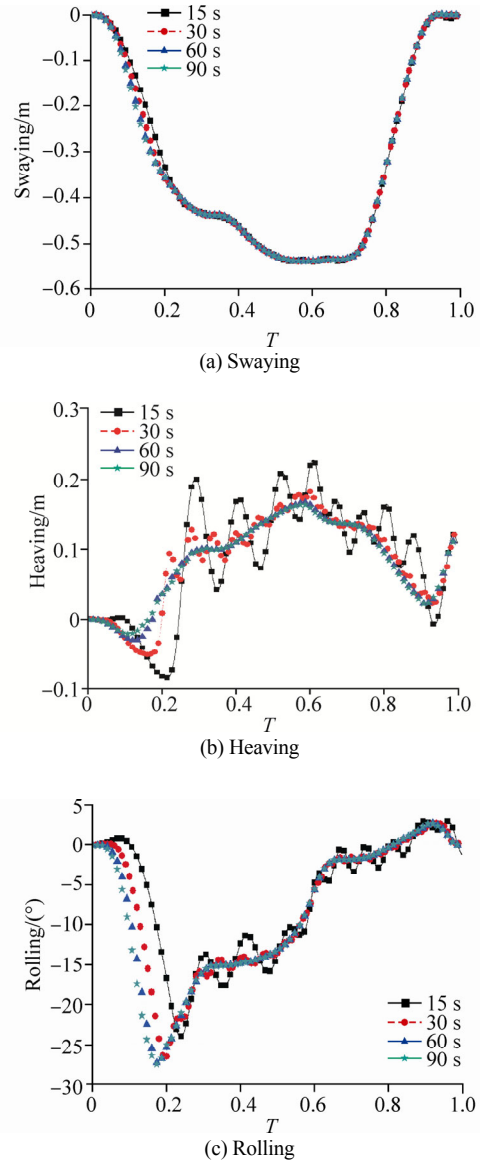


Fig. 3 Temporal variation of the floating base with sequential spreading

The temporal swaying variation of the floating base is shown in Fig. 4(a) when the upper parts spread synchronously on the static water surface. Fig. 4(a) demonstrates that the maximum swaying displacement of the floating base is about 0.53 m and the spreading time has less influence on it. The maximum value is presented near the location when the rigid body 4 spreads entirely, which is similar with the previous case with sequential spreading.

The temporal heaving variation of the floating base is shown in Fig. 4(b). It shows that the positive maximum heaving displacements are 0.210 m and 0.137 m and the negative ones are -0.074 m and -0.017 m when the upper parts spread in 15 s and 90 s, respectively. The difference of the heaving results of spreading in 60 s and 90 s is not distinct. It indicates that the inertial force has less influence on the spreading process and on the dynamic responses

when the spreading time is longer. Otherwise, comparing the synchronous heaving with the sequential one can demonstrate that the synchronous heaving value is less than the sequential one when the spreading time is long.

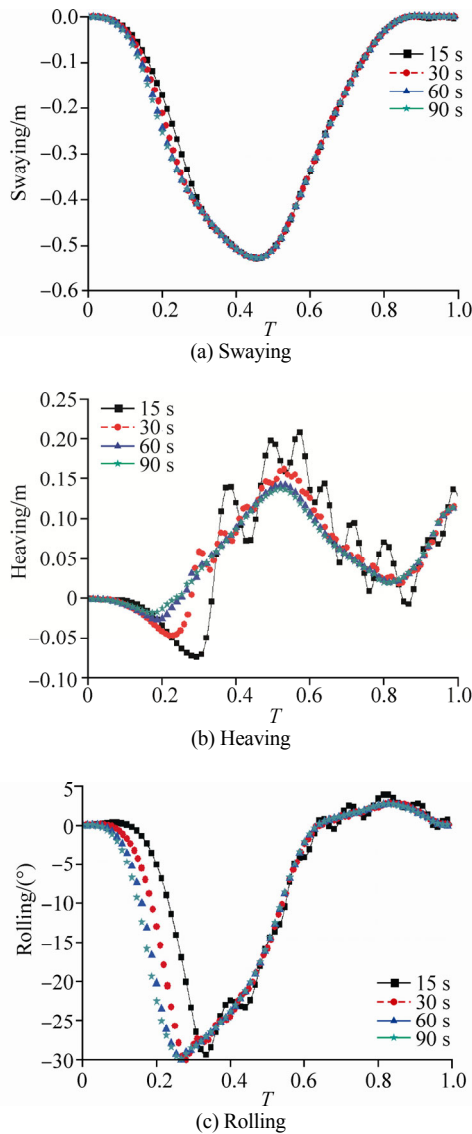


Fig. 4 Temporal variation of the floating base with synchronous spreading

The temporal rolling variation of the floating base is shown in Fig. 4(c) and it shows that the maximum rolling angle is presented when the rigid body 4 and joint part 3 spread on the half of the total time with respect to rigid 1. The longer the spreading time is, the smoother the rolling responses are. However, the maximum values of the rolling angle just have little difference, and they are about negative 30°.

5 Numerical results in waves

The numerical results in waves show the following: ① the rolling motion of the floating base is small, ② the

heaving motion of the floating base is vertical to the wave direction, namely the spreading motion of the multibody system is under the condition of beam sea and ③ the wave form is sinusoidal wave. On these basic supposes, the equation of the wave surface angle can be written as:

$$\alpha = \alpha_0 \cos \frac{t}{\tau_b} 2\pi \quad (24)$$

where α is instantaneous wave surface angle, α_0 the maximum wave surface angle and τ_b the wave period. So the periodic wave disturbing torques acting on the multibody system is as follows:

$$M_b = DgGM\alpha_0 \cos \frac{t}{\tau_b} 2\pi \quad (25)$$

The force matrix Φ_{FWA_i} ($i=1,2,3,4$) may be generated in Eq. (9) considering the wave disturbing torque as Eq. (25). Substitute it to Eq. (23) can obtain the dynamic response of the multibody system with a floating base spreading on waves, and the dynamic equation is as follows:

$$\text{skew} \left(H_{0,1}^* \cdot J_{1(0)} + H_{0,2}^* \cdot J_{2(0)} + H_{0,3}^* \cdot J_{3(0)} + H_{0,4}^* \cdot J_{4(0)} \right) - \sum_{i=1}^4 \left(\Phi_{FS_i} + \Phi_{FB_i} + \Phi_{FD_i} + \Phi_{FWA_i} + \Phi_{gr} \right) = \text{skew} \left(-\dot{W}_{0,1} \cdot J_{tot} \right) \quad (26)$$

The dynamic numerical simulations of the spreading of multibody system with a floating base will be under the conditions of three different wave periods ($\tau_b=3, 4$ and 5 s) and five different wave heights ($\zeta_w=0.2, 0.4, 0.6, 0.8$ and 1.0 m). Investigation on the spreading order of the multibody system acted by the waves, some suggestions would be obtained when the multibody system spreads in the wave conditions.

The temporal rolling variation of the floating base with fast spreading (entire spreading in 15 s) are shown in Fig. 5 when the wave period are $\tau_b=3, 4$ and 5 s, respectively. There are five wave heights including $\zeta_w=0.2$ m, 0.4 m, 0.6 m, 0.8 m and 1.0 m in the Fig. 6.

The temporal rolling variation of the floating base with slow spreading (entire spreading in 60 s) are shown in Fig. 6 when the wave period are $\tau_b=3$ s, 4 s and 5 s, respectively.

6 Numerical results acted by the wind loads

The dynamic response of the multibody system with a floating base acted by the wind load is considered below. The calculating equation of the force of the transverse mean wind is as follows:

$$P_f = PA \quad (27)$$

where P_f is transverse wind force, A is the wind pressure area vertical to the wind direction and P is wind pressure. The wind pressure P may be calculated according to the equation as follows (Yuan *et al.*, 2007):

$$P = \frac{1}{2} \rho c_p v^2 = 0.625 \rho v^2 \quad (28)$$

where v is the mean transverse wind velocity and the coefficient of the wind pressure $c_p=1.25$.

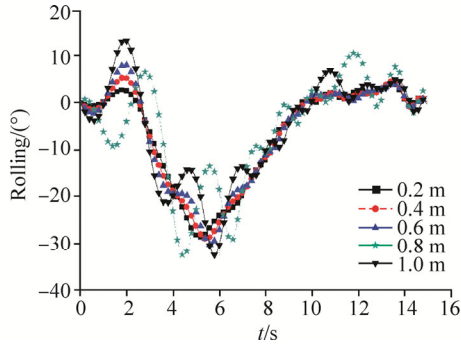
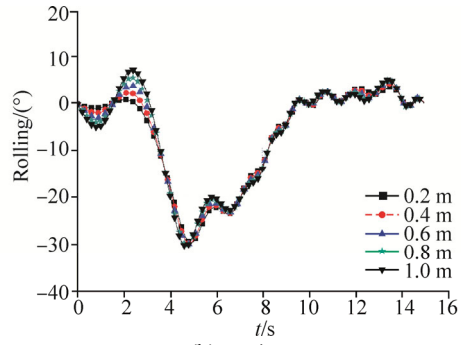
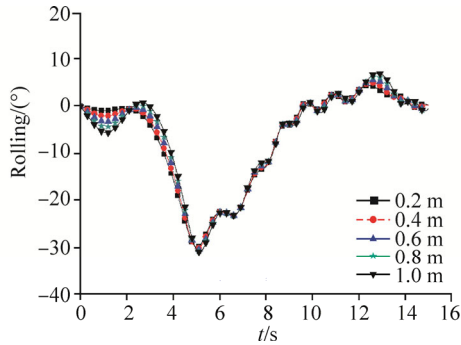
(a) $\tau_b=3$ s(b) $\tau_b=4$ s(c) $\tau_b=5$ s

Fig. 5 Temporal rolling variation of the floating base with fast spreading

The single pulse wind using the linear filter method (the autoregression AR method) was simulated and its formula is as follows:

$$v(t) = \sum_{k=1}^p \psi_k v(t - k\Delta t) + \sigma_N N(t) \quad (29)$$

where $v(t)$ is the time serial of the wind velocity, p is the rank number of autoregressive, Δt is the interval time and ψ_k ($k=1, 2, \dots, p$) is the parameter of autoregression. Referencing to the generation program of the single pulse wind (Yuan *et al.*, 2007) the mean wind speed is 23.6 m/s at the standard height (10 m), the roughness parameter of the land is $k=0.03$ and the autoregression time interval is 0.001 s. The temporal variation of the single pulse wind velocity with time 15 s, 30 s and 60 s are shown in Fig. 7(a)–(c), respectively.

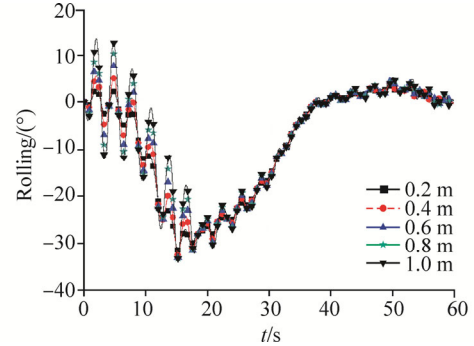
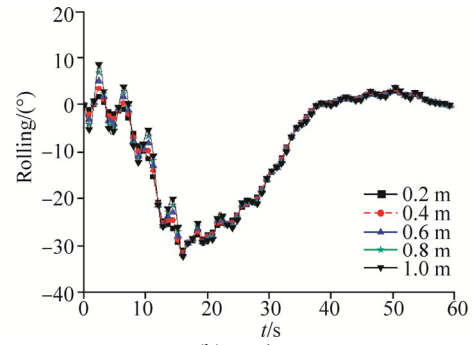
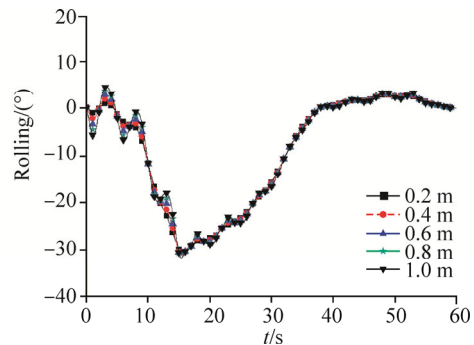
(a) $\tau_b=3$ s(b) $\tau_b=4$ s(c) $\tau_b=5$ s

Fig. 6 Temporal rolling variation of the floating base with slow spreading ($\tau_b=3$ s)

The force matrix Φ_{FWI_i} ($i=1,2,3,4$) may be generated by employing Eq. (9) considering the wave disturbing torque in Eq. (27). Substitute it to Eq. (23) can obtain the dynamic response of the multibody system subjected to wind loads and the dynamic equation is as follows:

$$\text{skew}(\mathbf{H}_{0,1}^* \cdot \mathbf{J}_{1(0)} + \mathbf{H}_{0,2}^* \cdot \mathbf{J}_{2(0)} + \mathbf{H}_{0,3}^* \cdot \mathbf{J}_{3(0)} + \mathbf{H}_{0,4}^* \cdot \mathbf{J}_{4(0)}) - \sum_{i=1}^4 (\Phi_{FS_i} + \Phi_{FB_i} + \Phi_{FD_i} + \Phi_{FWI_i} + \Phi_{gi}) = \text{skew}(-\dot{\mathbf{W}}_{0,1} \cdot \mathbf{J}_{tot}) \quad (30)$$

6.1 The dynamic response subjected to the mean wind load

The comparisons of the temporal swaying, heaving and rolling variant of the multibody system subjected to various wind scales are as Figs. 8–10 when the upper parts spread in 15, 30 and 60 s, respectively.

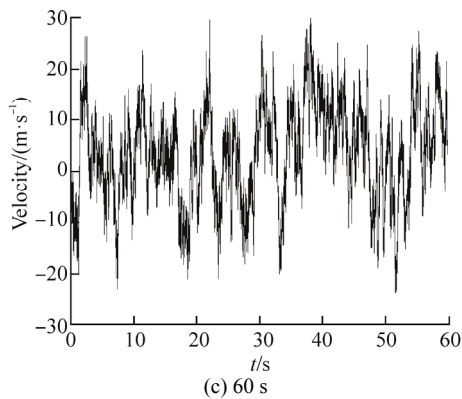
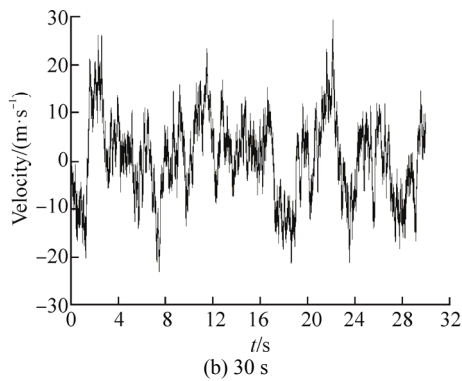
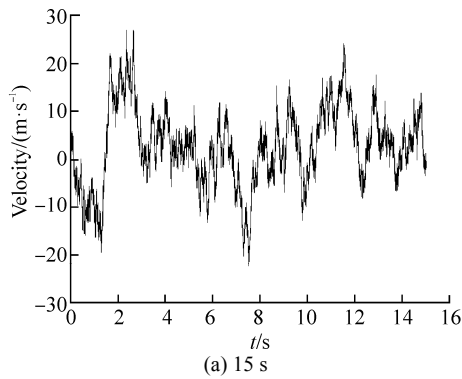


Fig. 7 Temporal variation of the single pulse wind velocity

Considering the temporal swaying variations subjected to no wind load as seen in Fig. 8(a), Fig. 9(a) and Fig. 10(a) can show that the floating base goes back to the round primary position when upper parts have spread completely. The results are coincident with the engineering practice. However, the swaying is larger when the wind scale subjected to the multibody system is higher. The ultimate swaying response of the floating base is listed in Table 3 when the upper parts spread under the conditions of different wind scales. The swaying displacement exceeds to 30 m when the multibody system are subjected to wind scale 6.

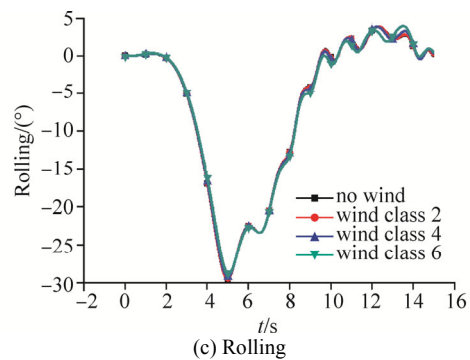
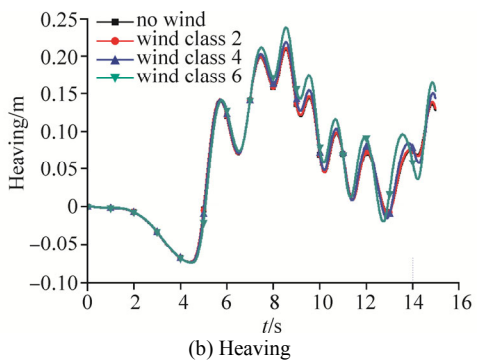
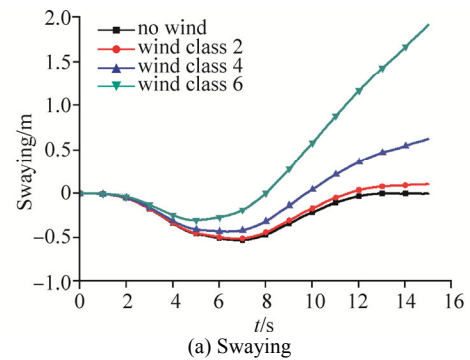


Fig. 8 Temporal variation of the dynamical response with spreading in 15 s

When considering the temporal heaving variations as shown in Fig. 8(b), Fig. 9(b) and Fig. 10(b) they can demonstrate that the impact of the wind scales on the heaving is distinct though it is less than that on the swaying. The longer the spreading time is, the larger the impacts are. For instance, the heaving displacement increases to about 0.35m under wind scale 6 while about 0.15 m under no wind loads with spreading in 60 s. Also, considering the temporal rolling variations, the figures demonstrate that although the different wind scales have some influences on the rolling angle, which impact is smaller and can be ignored. The maximum rolling angle of the floating base is negative 30.2° under no wind load, while it is negative 30.9° under the wind scale 6.

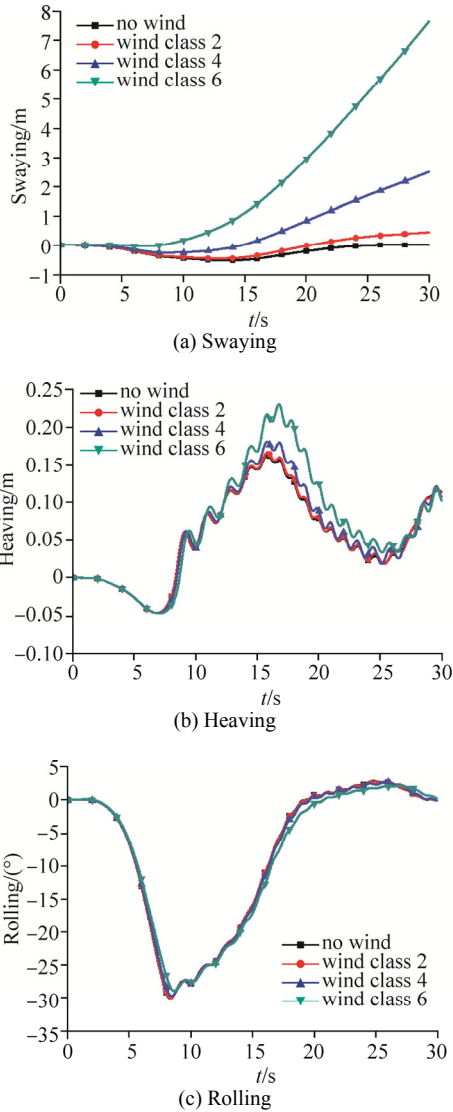


Fig. 9 Temporal variation of the dynamical response with spreading in 30 s

Table 3 Swaying responses when the multibody system spreads in different wind scales

Spreading time/s	wind scale			
	0	2	4	6
15	0	0.1	0.6	1.9
30	0	0.5	2.5	7.6
60	0	1.8	10.1	30.7

6.2 Dynamic responses subjected to the single pulse wind load

The comparisons of the temporal swaying, heaving and rolling variations of the floating base spreading under the conditions of no wind and single pulse wind are shown in Fig. 11. The whole spreading time is 5 s under the conditions of no wind load, while under the single pulse wind load, the total spreading time is 15 s, 30 s and 60 s, respectively.

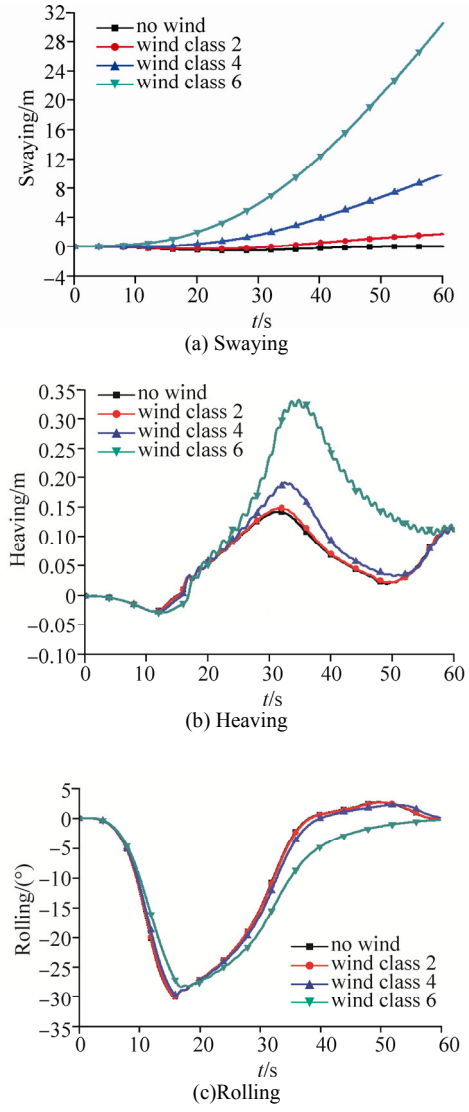


Fig. 10 Temporal variation of the dynamical response with spreading in 60 s

Fig. 11 demonstrates that the swaying, heaving and rolling of the floating base are distinctly affected by the pulse wind load. The influence of the pulse wind load on the spreading dynamic response of the multibody system is random. But on the whole, there are some rules similar to the mean wind load in the floating base actions. It is also noted that the dynamic responses of the swaying and the heaving under the pulse wind load are quite different to the other wind load forms when the spreading time is longer (such as 60 s).

The comparisons of the joint torques of the multibody system subjected to no wind load and single pulse wind load are shown in Fig. 12. Similarly, the whole spreading time is 15 s under the conditions of no wind load and the whole spreading time is 15 s, 30 s and 60 s under the conditions of the single pulse wind load, respectively.

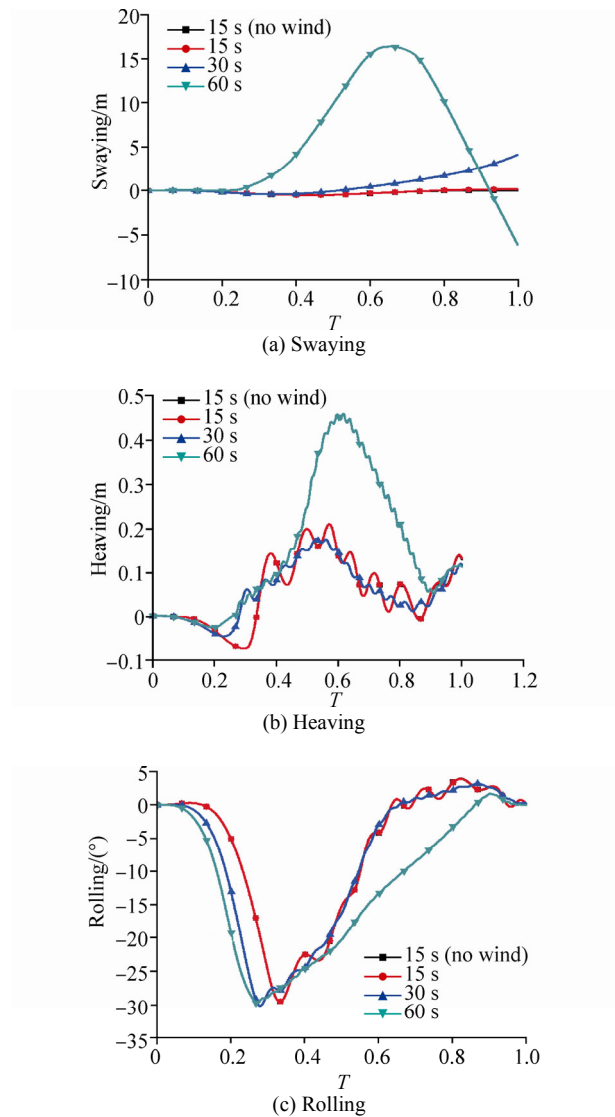


Fig. 11 Temporal variation of the dynamical response with various wind loads

The torques M_2 , M_3 and M_4 of the pulse wind time course of 15 s and 30 s are not identical according to Fig. 12. The maximum and minimum values of the torques of joint M_3 and M_4 are listed in Table 4 when the multibody spreads under the conditions of pulse wind load with time course of 15 s, 30 s and 60 s and the unit of torque is kN·m, respectively. Table 4 show that the variations of the torques of M_3 and M_4 under the conditions of time course of 60 s have many differences.

Table 4 Maximum values of torques M_3 and M_4 with spreading in different wind velocities

Torque	Temporal wind velocity			
	15 s	30 s	60 s	
M_3	Max.	134.4	135.9	123.1
	Min.	-74.8	-74.8	-284.3
M_4	Max.	79.1	75.6	70.7
	Min.	-75.4	-74.8	-181.2

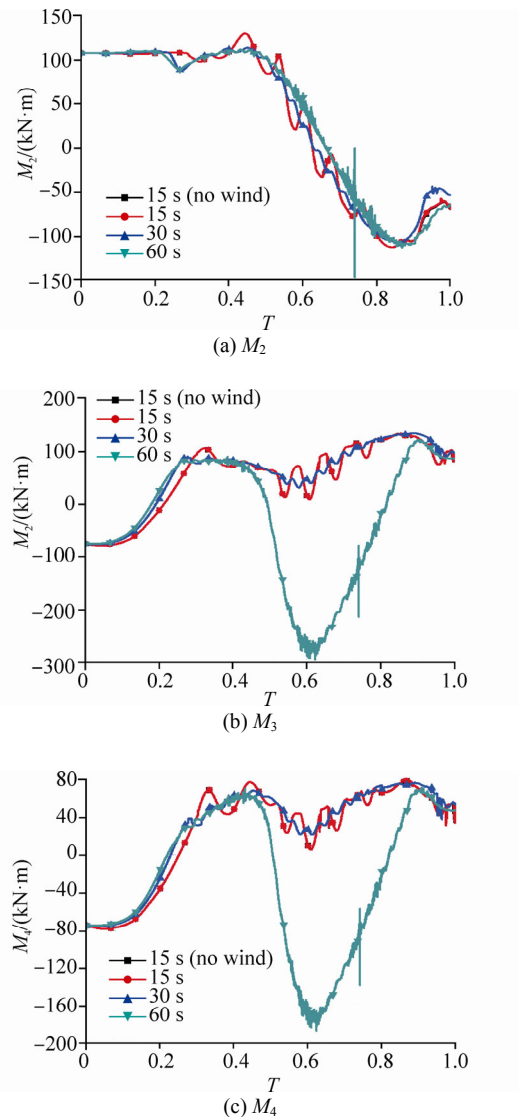


Fig. 12 Temporal variations of the torques with various wind loads

7 Conclusions

The self-exciting dynamic responses will be presented due to the large-angle spreading of the upper parts when the multibody system with a floating base spreads on the static water surface. The spreading form and time of upper parts may affect the dynamic responses of the system. The results of numerical simulation showed that the swaying of the floating base is almost not influenced by the spreading time and forms with sequential or synchronous order. However, the rolling and heaving obviously depends on the spreading time and form.

The total time for spreading are 15 s and 60 s under 15 wave cases based on the analysis of the rolling responses of the floating base with different spreading time, respectively. The results showed that the maximum rolling angle is positive relevant with the wave height and the same period wave, i.e., the larger the wave height is, the larger the maximum rolling angle is. The maximum rolling angle

under long period wave is less than that under short period wave.

According to the rolling dynamic response of the multibody system spreading in long time, the rolling response in the waves is correspondingly tempestuous and the reason is that the wave period is shorter than the spreading time. Comparing the slow spreading and the fast one, the maximum rolling response of slow spreading response is larger than the latter one. The result also showed that the spreading in short time may make the wave less influence on the rolling response.

There is less influence on the rolling response with longer wave period and the higher the wave amplitude is, the more the influence on the rolling response is. Generally, the spreading of the multibody system is unstable under the 0.6 m wave amplitude and more.

The response of the floating base is not violent with long spreading time under conditions of the same wind scale. The reason is that the longer the spreading time is, the less the inertial force is. The variation of the wind scale has large influence on the swaying of the floating base and there is some influence on the heaving and rolling, but the amplitude is relatively less.

The variations of the swaying and heaving of the multibody system are large amplitude under the single pulse wind load. The random of the dynamic response is various because the amplitude and the direction of the wind load are random. The violent variations of the torques of M_3 and M_4 reflect the dynamic characteristics of the pulse wind load. The results showed that the driving torque between rigid body 1 and 3 and the one between rigid body 3 and 4 are much larger under temporal wind variation when the multibody system spreads in 60 s than those under no wind.

References

- Cha JH, Roh MI, Lee KY (2010). Dynamic response simulation of a heavy cargo suspended by a floating crane based on multibody system dynamics. *Ocean Engineering*, **37**(14-15), 1273-1291.
DOI: 10.1016/j.oceaneng.2010.06.008
- de Wilde J, Serraris JJ, de Ridder EJ, Becel ML, Fournier JR (2010). Model test investigation of LNG tandem offloading with dynamic positioned shuttle tankers. *ASME*, Shanghai, 453-460.
DOI: 978-0-7918-4909-5
- Denavit J, Hartenberg RS (1955). A kinematics notation for lower-pair mechanisms based on matrices. *Trans. ASME J. Appl. Mech.*, **22**, 215-221.
- Dostal L, Kreuzer E (2013). Surf-riding threshold of ships in random seas. *Proceedings in Applied Mathematics and Mechanics*, **13**(1), 383-384.
DOI: 10.1002/pamm.201310187
- Du NJ, Shen YG, Zhang JH (2014). The dynamic response analysis of the multi-body system with Floating base based on the ADAMS. *Applied Mechanics and Materials*, **574**, 58-61.
DOI: 10.4028/www.scientific.net/AMM.574.58
- Ellermann K, Kreuzer E (2003). Nonlinear dynamics in the motion of floating cranes. *Multibody System Dynamics*, **9**(4), 377-387.
DOI: 10.1023/a:1023361314261
- Ellermann K, Kreuzer E, Markiewicz M (2002). Nonlinear dynamics of floating cranes. *Nonlinear Dynamics*, **27**(2), 107-183.
DOI: 10.1023/a:1014256405213
- Hu C, Kashiwagi M (2008). A CFD approach for extremely nonlinear wave-body interactions: development and validation. *IUTAM Symposium on Fluid-Structure Interaction in Ocean Engineering*, Hamburg, **8**, 129-140.
DOI: 10.1007/978-1-4020-8630-4_12
- Jang JH, Kwon SH, Jeung ET (2012). Pendulation reduction on ship-mounted container crane via T-S fuzzy model. *Journal of Central South University of Technology*, **19**(1), 163-167.
DOI: 10.1007/s11771-012-0986-5
- Jiang Z, Shen Q, Chen X, Zhao H (2010). Study on the application of the homogeneous matrix method of the multi-body system to the dynamic response of floating bridge. *Chinese Journal of Computational Mechanics*, **27**(6), 1036-1041. (in Chinese)
- Kim BW, Sung HG, Kim JH, Hong SY (2013). Comparison of linear spring and nonlinear FEM methods in dynamic coupled analysis of floating structure and mooring system. *Journal of Fluids and Structures*, **42**, 205-227.
DOI: 10.1016/j.jfluidstructs.2013.07.002
- Kim JH, Kim Y (2014). Numerical analysis on springing and whipping using fully-coupled FSI models. *Ocean Engineering*, **91**(15), 28-50.
DOI: 10.1016/j.oceaneng.2014.08.001
- Kral R, Kreuzer E (1999). Multibody systems and fluid-structure interactions with application to floating structures. *Multibody System Dynamics*, **3**(1), 65-83.
DOI: 10.1023/a:1009710901886
- Kreuzer E, Pick MA, Rapp C, Theis J (2014). Unscented Kalman filter for real-time load swing estimation of container cranes using rope forces. *Journal of Dynamic Systems Measurement and Control-Transactions of the ASME*, **136**(4), 121-130.
DOI: 10.1115/1.4026602
- Kreuzer E, Wilke U (2002). Mooring systems—A multibody dynamic approach. *Multibody System Dynamics*, **8**(3), 279-297.
DOI: 10.1023/a:1020917529011
- Lee I, Choi H (2015). A discrete-forcing immersed boundary method for the fluid-structure interaction of an elastic slender body. *Journal of Computational Physics*, **280**(1), 529-546.
DOI: 10.1016/j.jcp.2014.09.028
- Legnani G, Casolo F, Righettini P, Zappa B (1996a). A homogeneous matrix approach to 3D kinematics and dynamics. Part2: applications. *Mechanisms and Machine Theory*, **31**(5), 589-605.
- Legnani G, Casolo F, Zappa B, Righettini P (1996b). A homogeneous matrix approach to 3D kinematics and dynamics Part1: theory. *Mechanisms and Machine Theory*, **31**(5), 573-587.
- Li H, Shun P, Ren H, Wang Y (2013). Dynamic coupling analysis of mooring systems for a spar platform in time-varying wind. *Journal of Huazhong University of Science and Technology (Natural Science Edition)*, **41**(2), 36-40. (in Chinese)
DOI: 10.13245/j.hust.2013.02.020
- Rui XT, Kreuzer E, Rong B, He B (2012). Discrete time transfer matrix method for dynamics of multibody system with flexible beams moving in space. *Acta Mechanica Sinica (English Series)* **28**(2), 490-504.
DOI: 10.1007/s10409-012-0025-7
- Shen Q, Li Y, Chen X J (2003). Dynamic analysis of multibodies system with a floating-base for rolling of ro-ro ship caused by wave and slip of heavy load. *Journal of Marine Science and Application*, **2**(2): 17-24.
DOI: 10.1007/BF02918659

- Surendran S, Lee SK, Reddy JVR, Lee G (2005). Non-linear roll dynamics of a ro-ro ship in waves. *Ocean Engineering*, **32**(14-15), 1818-1828.
DOI: 10.1016/j.oceaneng.2004.11.014
- Wang Q, Sun LP, Ma S (2010). Time-domain analysis of FPSO-tanker responses in tandem offloading operation. *Journal of Marine Science and Application*, **9**(2), 200-207.
DOI: 10.1007/s11804-010-9070-4
- Woodburn P, Gallagher P, Ferrant P, Borleteau JP (2003). EXPRO-CFD: Development and validation of CFD based co-simulation of spar/CALM buoy fluid structure interaction. In: Chung JS, Wardenier J, Frederking RMW, Koterayama W. eds. *Proceedings of the Thirteenth International Offshore and Polar Engineering Conference*, Honolulu, USA, 175-181.
- Xia D, Ertekin RC, Kim JW (2008). Fluid-structure interaction between a two-dimensional mat-type VLFS and solitary waves by the Green-Naghdi theory. *Journal of Fluids and Structures*, **24**(4), 527-540.
DOI: 10.1016/j.jfluidstructs.2007.10.009
- Yuan B, Ying HQ, Xu JW (2007). Simulation of turbulent wind velocity based on linear filter method and MATLAB Program Realization. *Structural Engineers*, **23**(4), 55-61.
DOI: 10.15935/j.cnki.jggcs.2007.04004
- Zhang J, Zhang K, Zhou A, Zhou T, Hu D, Ren J (2014). Analysis of nonlinear dynamic response of wind turbine blade under fluid-structure interaction and turbulence effect. *Journal of Engineering for Gas Turbines and Power—Transactions of the ASME*, **136**(10): 26-30.
DOI: 10.1115/1.4027965
- Zhang RY, Chen CH, Tang YG (2012). Study on the dynamic characteristic for spar type floating foundation of offshore wind turbine. *Applied Mechanics and Materials*, **170-173**, 2316-2321.
DOI: 10.4028/www.scientific.net/AMM.170-173.2316
- Zhang YL, Shen Q, Chen XJ (2006). Synchronous effect of slipping heavy loads on ro-ro ship rolling in waves. *Applied Mathematics and Mechanics (English Edition)*, **27**(7), 959-966.
DOI: 10.1007/s10483-006-0712-y
- Zhao W, Yang J, Hu Z, Xie B (2013). Hydrodynamics of an FLNG system in tandem offloading operation. *Ocean Engineering*, **57**(1), 150-162.
DOI: 10.1016/j.oceaneng.2012.09.015
- Zhao WH, Yang JM, Hu ZQ, Tao LB (2014). Prediction of hydrodynamic performance of an FLNG system in side-by-side offloading operation. *Journal of Fluids and Structures*, **46**, 89-110.
DOI: 10.1016/j.jfluidstructs.2013.11.021